Plasmon Dispersion of the Au(111) Surface with and without Self-Assembled Monolayers

Sung Jin Park and Richard E. Palmer

Nanoscale Physics Research Laboratory, School of Physics and Astronomy, University of Birmingham, Edgbaston, Birmingham, B15 2TT, United Kingdom

(Received 11 December 2008; published 29 May 2009)

The surface plasmon dispersion of gold films with and without chemisorbed, alkane thiol self-assembled monolayers (SAMs) has been investigated using high resolution electron energy loss spectroscopy (HREELS). For a bare Au(111) film, the surface plasmon energy (2.49 eV at the zone center) shows a positive dispersion. After adsorption of ethylbenzenethiol or dodecanethiol SAMs, the plasmon energy at the zone center blueshifts and the dispersion switches sign to become negative, thus mimicking the behavior of a free-electron system. This striking behavior represents a benchmark for models of the electronic structure of the gold-sulfur interface, as manifest both in SAMs and in monolayer-protected nanoparticles.

DOI: 10.1103/PhysRevLett.102.216805 PACS numbers: 73.20.Mf, 68.43.Fg, 79.20.Uv, 81.16.Dn

There is considerable interest, both experimental and theoretical, in understanding the electronic excitations which control the response of a metal surface to external stimuli [1–8]. The dispersion of the surface plasmon energy as a function of momentum parallel to the surface ($q_{\parallel}$) manifests the fundamental nature of the charge screening by the surface [4,8]. Similar considerations apply to metal cluster plasmons as a function of cluster size [5,7]. Free-electron metals [3,8] show a negative dispersion at small $q_{\parallel}$ ($<\sim 0.15$ Å^{-1}), but Ag [4,6] shows a positive dispersion as well as a large redshift in the plasma frequency at $q_{\parallel} = 0$ compared with that expected from the free-electron model. Both effects are attributed to the screening of the *s* electrons by the *d* band charge density [4,6]. In this work we report the plasmon dispersion of the Au(111) surface, before and after addition of SAMs, thus illuminating the surface electronic structure of the planar sulfur-gold interface [9–12]. We relate the results to the sulfur-gold interface of thiol monolayer-protected nanoparticles [13–16] and develop a benchmark for models of the electronic structure of the gold-sulfur interface. Both the SAMs and the nanoparticles are currently prominent both in science and in applications [17] on the nanometer scale.

It is a curious fact that, although gold is exploited in the surface plasmon resonance sensors now used extensively in the biosciences [18], the plasmon dispersion of the Au surface has not been reported. Moreover, the nature of the bonding of SAMs to the Au(111) surface is again a topic of lively debate [9–12]. Our HREELS measurements show that the surface plasmon dispersion of bare Au(111) is positive but the formation of SAMs blueshifts the plasmon energy at $q_{\parallel} = 0$ and causes the initial dispersion to switch sign, indicating a suppression of the screening of the *s* electrons by the gold *d* band in the new surface complex.

Gold films around 90 nm thick were grown on mica by thermal evaporation with the substrate temperature held at 350 °C. This procedure generates the low energy (111) surface [19,20] and produces large terraces a few hundred nanometers across, as observed in atomic force microscopy (AFM) images. The gold films were introduced into an ultrahigh vacuum (UHV) chamber and sputtered using Ar^+ ions (500 V, 1 μA, 10 min), followed by annealing at about 400 °C (30 min). Several cycles were employed to obtain a clean surface. The surface plasmon measurements were performed using an (LK3000) HREELS instrument. For these bare Au films, the incident energy was 20 eV and the detection angle set at 60° or 70° with respect to the surface normal (the monochromator is rotatable). Two kinds of SAMs (4-ethylbenzenethiol [$HS(C_6H_4)CH_2CH_3$] and dodecanethiol [$HS(CH_2)_{11}CH_3$] were prepared by immersion of similar gold films in 1 mM solutions for 24 h. After drying the samples in air, the surface plasmon measurements were carried out in UHV with incident energies in the range 32.5–40.0 eV and detection angle 60° with respect to the surface normal.

Representative energy loss spectra showing the surface plasmon of the bare Au(111) surface are presented in Fig. 1 for different values of $q_{\parallel}$ (obtained by rotating the monochromator). The chosen energy resolution was normally 25 to 35 meV and the analyzer acceptance angle was 2.5°. Figure 1(a) is an example of the raw data together with a polynomial (in this case approximately linear) background fitted $\sim$1 eV either side of the peak base. After background subtraction, Fig. 1(b), the peak itself is fitted with an (asymmetric) modified Gaussian function. All the spectra in Fig. 1(b) show an asymmetric energy loss peak; the tail on the higher energy side is possibly associated with interband transitions.

Figure 2 displays the dispersion of the surface plasmon of the bare Au(111) surface, obtained from the fitted peak positions such as those shown in Fig. 1. The vertical (i.e., energy) error bars shown derive from the numerical fitting error; the scatter of the data points (see Fig. 4 below, for example) suggests a measurement error of up to about

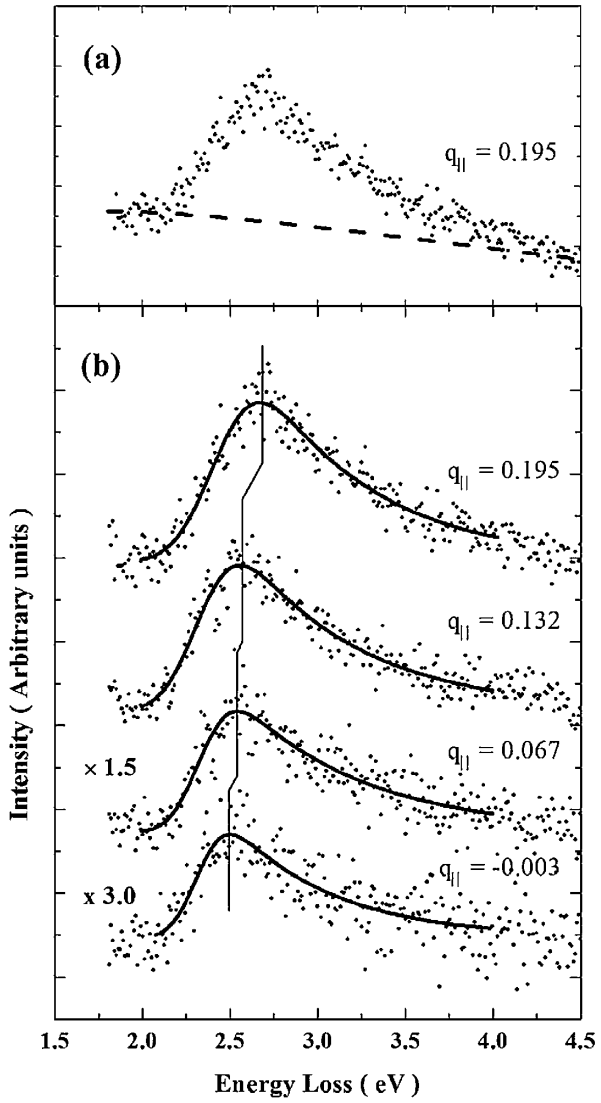

FIG. 1. Electron energy loss spectra from the bare Au(111) surface. (a) Example of raw data and background; (b) spectra for different values of parallel momentum transfer, $q_{\|}$, after background subtraction. The incident electron energy is 20 eV and detection angle 60° with respect to the surface normal. Each surface plasmon peak energy (and associated error bar) is determined by fitting the smoothed data to a modified (asymmetric) Gaussian function.

60 meV. The solid line is the best fit to the data of a second-order quadratic function, which is given by $\omega_{sp} = 2.49 + 0.40q_{\|} + 1.70q_{\|}^2$. It is evident from the data that the initial surface plasmon dispersion of Au(111) is positive. The dispersion of the Ag(111) surface plasmon is also positive and is explained by the *s*-*d* polarization model [6]. In this scheme, screening of the 5*s* electrons by the 4*d* band electrons explains the relatively low bulk and surface plasmon frequencies compared with the free-electron model. However, some of the 5*s* electrons spill out of the surface beyond the more confined 4*d* electrons; large values of $q_{\|}$ correspond to the higher frequency *s* electron

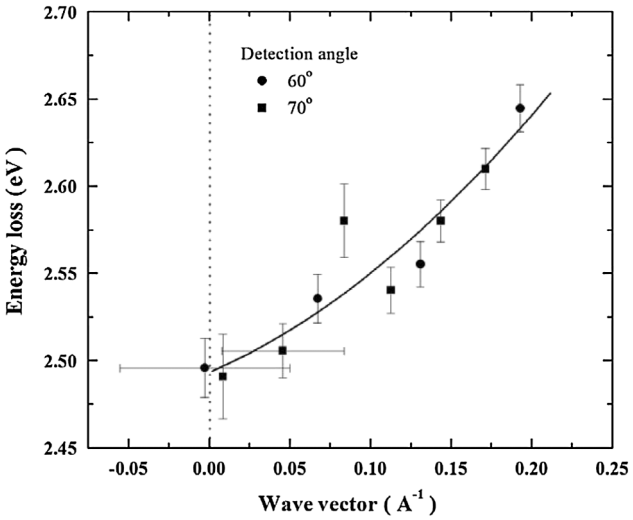

FIG. 2. Surface plasmon dispersion of the bare Au(111) surface as a function of parallel momentum transfer, $q_{\|}$. The incident electron energy is 20 eV and the detection angle 60° (circles) or 70° (squares) with respect to the surface normal. The solid line is the best parabolic fit to the data.

oscillations in this outer surface region. Our experimental results suggest that the same model holds good for gold (i.e., for its 6*s* and 5*d* electrons). The relatively low energy onset of the interband transitions in Au compared with Ag [21,22] does not seem to disturb this picture, but is reflected in an enhanced damping of the Au plasmon (the measured width from Fig. 1(b) is ~600 meV at $q_{\|} = 0$ for Au, but only ~100 meV for Ag [4]). Moreover, the measured surface plasmon energy for Au in Fig. 1(b) at the zone center (2.49 eV) is lowered by ~60% from the free-electron gas value (~6.4 eV [23]) by the *d* band screening. For Ag the shift is only ~40% [4]. This difference in the degree of screening is confirmed by thermalization measurements [24].

Figure 3 shows the surface plasmon dispersion for the 4-ethylbenzenethiol SAM on Au(111); the bare Au(111) result is reproduced for comparison. Two notable changes are induced by adsorption of the SAM. First, the initial dispersion switches from positive to negative slope at small $q_{\|}$ (<0.13 Å^{-1}). Secondly, the plasmon energy at $q_{\|} = 0$ shifts from 2.49 eV for bare Au to 2.64 eV when the SAM is adsorbed. Both effects are consistent with an enhanced degree of free-electron behavior in the gold surface layer. The best quadratic fit to the data is given by $\omega_{sp} = 2.64 - 0.45q_{\|} + 1.73q_{\|}^2$. Figure 4 presents the dispersion of a second SAM, an annealed [25] dodecanethiol monolayer on the Au(111) surface. The experimental results, fitted by the quadratic function $\omega_{sp} = 2.62 - 0.26q_{\|} + 0.90q_{\|}^2$, show exactly the same trends as the first SAM—a negative dispersion at small $q_{\|}$ and a blueshift of the surface plasmon energy at $q_{\|} = 0$ (to 2.62 eV). We conclude that the significant changes in the behavior of the Au(111) surface

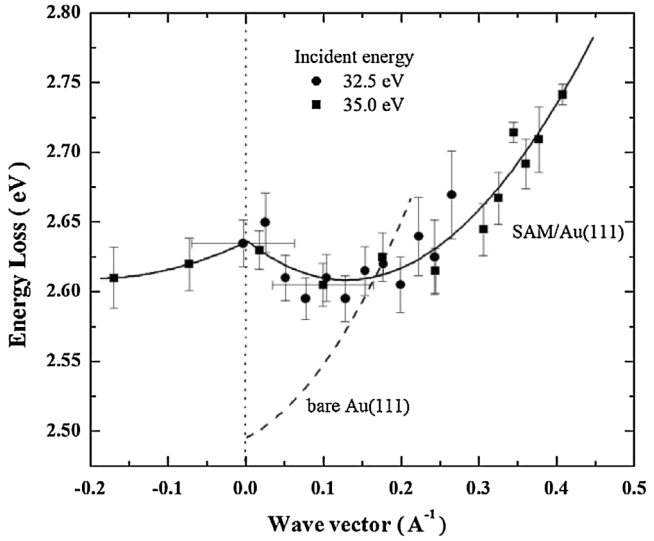

FIG. 3. Surface plasmon dispersion of a 4-ethylbenzenethiol self-assembled monolayer on Au(111). The incident electron energies employed are 32.5 eV (circles) and 35.0 eV (squares) and the detection angle is 60° with respect to the surface normal. The solid lines represent the best parabolic fits to the data (for positive and negative values of $q_{\|}$). For comparison the surface plasmon dispersion of bare Au(111) is also presented (dashed line, from Fig. 2).

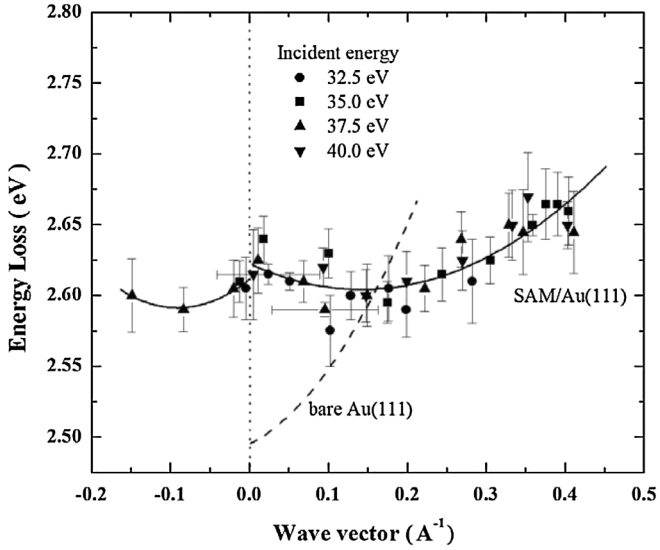

FIG. 4. Surface plasmon dispersion of a dodecanethiol SAM on Au(111). The incident electron energies employed are 32.5 eV (circles), 35.0 eV (squares), 37.5 eV (upward-pointing triangles) and 40.0 eV (downward-pointing triangles) and the detection angle is 60° with respect to the surface normal. The solid lines represent the best parabolic fits to the data (for positive and negative values of $q_{\|}$). For comparison the surface plasmon dispersion of bare Au(111) is also presented (dashed line, from Fig. 2).

plasmon upon adsorption of the SAMs depend mainly on the local electronic structure [26,27] at the sulfur-gold interface, rather than on the electronic structure of the molecular chain.

The dispersion of the surface plasmon of the SAM-Au(111) system represents a new and sensitive probe of the atomic or electronic structure of the sulfur-gold interface. Ideally, one would like to compare the measured plasmon dispersion with the competing theories of bonding via first-principles calculations of the surface plasmon dispersion based on the particular atomic models [9,11] of the interface, e.g., the formation of gold-sulfur complexes on top of the Au(111) surface [11]. In the absence to date of first-principles calculations of surface plasmon dispersion—except for a few elemental surfaces [3,4]—we focus attention on those features arising from the experiment (explicitly and implicitly) which the bonding models will need to account for.

Recent x-ray diffraction measurements of thiol-passivated gold nanoclusters reveal a gold core surrounded by gold-containing thiolate complexes [15,16], while first-principles electronic structure calculations [13] expose the electron counting rules and closed electronic shells (magic numbers) which stabilize these structures. Relevant to the planar interface is the conclusion that the gold-thiolate complexes cause 6*s* electron localization and withdrawal (a polarized covalent bond is formed) from the gold core (at the rate of one 6*s* electron per adsorbed complex). This feature is (qualitatively) consistent with mainstream views of SAM bonding to planar Au, and if replicated at the Au(111) surface, such bonding would remove the low density tail of the surface 6*s* electron spillout from the surface plasmon [26]. The mean 6*s* electron density associated with the plasma oscillation would therefore be higher and—if we set aside for a moment *d* band screening—the zone center surface plasmon frequency would blueshift (as observed). However, once we add in the type of *d* band screening discussed earlier, we realize that curtailing the *s* electron spillout would actually tend to redshift the surface plasmon energy via enhanced 5*d* band screening (assuming no change in the *d* band confinement). Therefore, if our reasoning is correct, the experimental blueshift requires of the bonding theory that the 5*d* bands of the gold surface must also be modified by the SAM. Indeed, reported ultraviolet photoelectron spectroscopy (UPS) measurements of octanethiol [$CH_3(CH_2)_7SH$] monolayers on Au(111) [28] do suggest a modest shift in the density of the Au 5*d* band states to deeper energies. If such a shift were associated (reasonably) with increased localization of the *d* band electrons, thereby reducing the interband screening of the 6*s* electron plasmon, a blueshift of the surface plasmon frequency at the zone center could follow, together with a switch to the negative initial dispersion characteristic of *s* electrons which are more free (i.e., less strongly screened by the *d* band) [4], i.e., the two principal features observed experimentally could both be accounted for. These new measurements thus present a

challenge to quantitative models of the SAM structure and bonding at two levels: (i) they have to predict the right kind of screening behavior, and (ii) ultimately they need to reproduce both the blueshift and the negative dispersion of the surface plasmon.

In summary, we have presented experimental studies of the surface plasmon dispersion for Au(111) and for SAMs on Au(111) using HREELS. The results show two important changes arising from the adsorption of SAMs. First, the positive dispersion of the surface plasmon observed on the bare Au(111) surface switches sign upon attachment of the SAMs. Secondly, the surface plasmon energy at $q_{\parallel} = 0$ blueshifts (a little) towards the ''free-electron'' surface value. Both effects could in principle be explained by the reduction of the Au 5*d* band screening of the 6*s* electron surface plasmon oscillations, such that the gold surface layer acquires an enhanced free-electron metal character. These results will present a searching benchmark for quantitative theories of the bonding at the (ubiquitous) Au-SAM interface.

We thank the EPSRC for financial support of this work.

[1] G. P. Wiederrecht, J. E. Hall, and A. Bouhelier, Phys. Rev. Lett. **98**, 083001 (2007).
[2] T. Nagao, S. Yaginuma, T. Inaoka, and T. Sakurai, Phys. Rev. Lett. **97**, 116802 (2006).
[3] V. M. Silkin, E. V. Chulkov, and P. M. Echenique, Phys. Rev. Lett. **93**, 176801 (2004).
[4] M. Rocca, Surf. Sci. Rep. **22**, 1 (1995).
[5] J. Tiggesbäumker, L. Köller, K. H. Meiwes-Broer, and A. Liebsch, Phys. Rev. A **48**, R1749 (1993).
[6] A. Liebsch, Phys. Rev. Lett. **71**, 145 (1993).
[7] C. Bréchignac, Ph. Cahuzac, N. Kebaili, J. Leygnier, and A. Sarfati, Phys. Rev. Lett. **68**, 3916 (1992).
[8] K.-D. Tsuei, E. W. Plummer, and P. J. Feibelman, Phys. Rev. Lett. **63**, 2256 (1989).
[9] A. Cossaro, R. Mazzarello, R. Rousseau, L. Casalis, A. Verdini, A. Kohlmeyer, L. Floreano, S. Scandolo, A. Morgante M. L. Klein, and G. Scoles, Science **321**, 943 (2008).
[10] R. Mazzarello, A. Cossaro, A. Verdini, R. Rousseau, L. Casalis, M. F. Danisman, L. Floreano, S. Scandolo, A. Morgante, and G. Scoles, Phys. Rev. Lett. **98**, 016102 (2007).
[11] H. Grönbeck, H. Häkkinen, and R. L. Whetten, J. Phys. Chem. C **112**, 15 940 (2008).
[12] M. Yu, N. Bovet, C. J. Satterley, S. Bengió, K. R. J. Lovelock, P. K. Milligan, R. G. Jones, D. P. Woodruff, and V. Dhanak, Phys. Rev. Lett. **97**, 166102 (2006).
[13] M. Walter, J. Akola, O. Lopez-Acevedo, P. D. Jadzinsky, G. Calero, C. J. Ackerson, R. L. Whetten, H. Grönbeck, and H. Häkkinen, Proc. Natl. Acad. Sci. U.S.A. **105**, 9157 (2008).
[14] J. Akola, M. Walter, R. L. Whetten, H. Häkkinen, and H. Grönbeck, J. Am. Chem. Soc. **130**, 3756 (2008).
[15] M. W. Heaven, A. Dass, P. S. White, K. M. Holt, and R. W. Murray, J. Am. Chem. Soc. **130**, 3754 (2008).
[16] P. D. Jadzinsky, G. Calero, C. J. Ackerson, D. A. Bushnell, and R. D. Kornberg, Science **318**, 430 (2007).
[17] M.-C. Daniel and D. Astruc, Chem. Rev. **104**, 293 (2004).
[18] E. Hutter and J. H. Fendler, Adv. Mater. **16**, 1685 (2004).
[19] V. M. Hallmark, S. Chiang, J. F. Rabolt, J. D. Swalen, and R. J. Wilson, Phys. Rev. Lett. **59**, 2879 (1987).
[20] C. E. D. Chidsey, D. N. Loiacono, T. Sleator, and S. Nakahara, Surf. Sci. **200**, 45 (1988).
[21] P. B. Johnson and R. W. Christy, Phys. Rev. B **6**, 4370 (1972).
[22] P. Winsemius, F. F. van Kampen, H. P. Lengkeek, and G. G. van Went, J. Phys. F **6**, 1583 (1976).
[23] This is calculated for the electron density of bulk Au, with $r_s = 3.01$; see C. Kittel, *Introduction to Solid State Physics* (John Wiley & Sons, Singapore, 1991), p. 134.
[24] N. Del Fatti, C. Voisin, M. Achermann, S. Tzortzakis, D. Christofilos, and F. Vallée, Phys. Rev. B **61**, 16 956 (2000).
[25] The dodecanethiol SAM sample was additionally annealed at ~100 °C for 1 h after preparation. It is reported [C. Schönenberger, J. Jorritsma, J. A. M. Sondag-Huethorst, and L. G. J. Fokkink, J. Phys. Chem. **99**, 3259 (1995)] that the annealing process increases the molecular domain size by about 10 times.
[26] J.-S. Kim, L. Chen, L. L. Kesmodel, P. García-González, and A. Liebsch, Phys. Rev. B **56**, R4402 (1997).
[27] F. Moresco, M. Rocca, T. Hildebrandt, and M. Henzler, Surf. Sci. **424**, 55 (1999).
[28] H. Rieley, N. J. Price, R. G. White, R. I. R. Blyth, and A. W. Robinson, Surf. Sci. **331–333**, 189 (1995).